



Radioprotective efficacy of zinc oxide nanoparticles on γ -ray-induced nuclear DNA damage in *Vicia faba* L. as evaluated by DNA bioassays

Ekram Abdelhaliem Mohamed, Hanan Fahad A. L. Harbi & Nagwa Aref

To cite this article: Ekram Abdelhaliem Mohamed, Hanan Fahad A. L. Harbi & Nagwa Aref (2019) Radioprotective efficacy of zinc oxide nanoparticles on γ -ray-induced nuclear DNA damage in *Vicia faba* L. as evaluated by DNA bioassays, *Journal of Radiation Research and Applied Sciences*, 12:1, 423-436, DOI: [10.1080/16878507.2019.1690798](https://doi.org/10.1080/16878507.2019.1690798)

To link to this article: <https://doi.org/10.1080/16878507.2019.1690798>



© 2019 The Author(s). Published by Informa UK Limited, trading as Taylor & Francis Group.



Published online: 25 Nov 2019.



Submit your article to this journal [↗](#)



Article views: 234






View related articles [↗](#)



View Crossmark data [↗](#)

Radioprotective efficacy of zinc oxide nanoparticles on γ -ray-induced nuclear DNA damage in *Vicia faba* L. as evaluated by DNA bioassays

Ekram Abdelhaliem Mohamed ^a, Hanan Fahad A. L. Harbi ^b and Nagwa Aref ^c

^aPlant Molecular Genetics, Botany and microbiology Department, Science College, Zagazig University, Zagazig, Egypt; ^bBotany and Microbiology Department, King Saud University, Riyadh, Saudi Arabia; ^cFaculty of Agriculture, Department of Microbiology, Ain Shams University, Cairo, Egypt

ABSTRACT

This study aimed to assess radioprotective efficacy of zinc oxide nanoparticles (nano-ZnO) against γ -radiation induced DNA lesions in *Vicia faba* employing flow cytometry (FCM), comet assay, and RAPD-PCR bioassays. Each dose of γ -irradiated seeds was post-treated with three nano-ZnO concentrations. Exposure time pre- and post-ZnO treatments were 24 h. Dose-dependent nano-ZnO and γ -ray treatments showed specific interference with DNA. Three bioassays could successfully detect positive action of two nano-ZnO concentrations (500 and 2000 mg L⁻¹) on DNA compared to control while high concentration nano-ZnO showed a negative interference with DNA. On the contrary, three doses of γ -ray induced major lesions in *V. faba* DNA. Data obtained illustrated that combination of 2000 mgL⁻¹ nano-ZnO concentration with each γ -ray dose had a good ability to protect DNA against their damaging when compared to the equivalent γ -ray doses prior nano-ZnO treatment. This was evident through the significant amelioration of DNA parameters which manifested in increasing nuclear DNA content and genome size, reduction the DNA damage (tail length, Tailed DNA% and tail moment), and scoring new amplified DNA bands and increasing their number. This study concluded that nano-ZnO can be used as potent mutant and an efficient nano-radioprotector for the protection of crop plants DNA.

ARTICLE HISTORY

Received 1 July 2019
Revised 9 October 2019
Accepted 5 November 2019

KEYWORDS

ZnO nanoparticle; ionizing gamma-radiation; DNA damages; radioprotective; DNA bioassays

1. Introduction

Broad bean (*Vicia faba*) is used as an important model system among the plant bioassays for monitoring environmental pollutants as reviewed by the US Environmental Protection Agency (EPA) Gene Tox program (Ma, Owens, & Cabrera, 2005). It has been used to study DNA damages such as chromosomal and nuclear aberrations induced by toxins, nanoparticles, and ionizing radiations. The *V. faba* test offers an evaluation of different endpoints and tested agents can be classified as cytotoxic/genotoxic/mutagenic (Iqbal, 2016). Therefore, the value of plant bioassay for monitoring and screening genotoxicity can be improved by greater knowledge of processes of plant cell at DNA levels.

Ionizing radiations are used to sterilize some agricultural products in order to increase their conservation time or to reduce pathogen propagation; this may exert adverse effects on plant growth, development, fertility, and crop production. Gamma rays are the most effective ionizing radiation, having high level of energy, therefore, they are the more penetrating, environmental exposure to gamma rays induces a greater degree of biological damage than exposure to alpha or beta particles (Reisz, Bansal, Qian, Zhao, & Furdui, 2014). The biological effect of gamma-rays in plant cells based on the mode of interaction with water atoms or DNA molecules in the

cell. It is a potent DNA-damaging agent, which interacts with cellular DNA by inducing oxidative stress with over production of free radicals, reactive oxygen species (ROS) (Reisz et al., 2014) through the direct and/or indirect effect on DNA to induce lesions and DNA breaks in the irradiated cells. This radiolytic ROS are highly reactive with cellular macromolecules, such as RNA, and DNA which includes base deletion, pyrimidine dimers, cross-links, strand breaks, and base modification, molecular alterations, improper segregation of chromosomes during mitosis (Nurmansyah, Alghamdi, Hussein, & Farooq, 2018; Caplin & Willey, 2018).

Protection against ionizing radiation is of serious importance during accidental and unavoidable exposures of economic crop plants to radiation. So, development of the effective approaches to reduce radiation damages using nontoxic radioprotectors is of considerable interest. Recently, the possible application of nanoparticles (NPs) in agricultural fields has been drawn much attention, owing to their unique bioactive, a high reactivity and their small size as well as they have a high specific area and a high surface energy that produce changes in its physicochemical, optical and electrical properties (Veronica, Guru, Thatikunta, & Reddy, 2015). The biological effect of these nanoparticles likely depends on the target plant tissue and the way of entry.

CONTACT Ekram Abdelhaliem Mohamed  ekram.esa@gmail.com  Botany and microbiology Department, Science College, Zagazig University, Zagazig, Egypt

© 2019 The Author(s). Published by Informa UK Limited, trading as Taylor & Francis Group.
This is an Open Access article distributed under the terms of the Creative Commons Attribution License (<http://creativecommons.org/licenses/by/4.0/>), which permits unrestricted use, distribution, and reproduction in any medium, provided the original work is properly cited.

Recently studies also showed radioprotective effect of various nanoparticles such as cerium oxide nanoparticles (NPs), zinc oxide (ZnO) NPs and carbon nanoparticles, etc., owing to they possess antioxidant properties and plays a key role in cellular defenses against oxidative DNA damage induced by ionizing radiations (Wang et al., 2016; Karami, Asri-Rezaei, Dormanesh, & Nazarizadeh, 2018; Liu et al., 2018, respectively).

ZnO nanoparticles (nano-ZnO) have become one of the most popular metal oxide nanoparticles in biological applications due to their excellent biocompatibility, economic, and low toxicity (Jiang, Pi, & Cai, 2018). Compared with other metal oxide NPs, Nano-ZnO with the comparatively inexpensive and relatively less toxic property exhibit excellent potential role as free radical scavengers and antioxidants, in biological systems (Siddiqi & Husen, 2017; Zafar, Ali, Ali, Haq, & Zia, 2016). More specifically, there is a growing interest in the use of nano-ZnO in agricultural formulations by either using their good properties as an ultraviolet light-blocking substance or using their fertilizer properties as a source of zinc micronutrient (Duhan et al., 2017). On the other hand, nano-ZnO has shown much better plant protection by its antimicrobial activity against many pathogenic (Xie, He, Irwin, Jin, & Shi, 2011). Additionally, the current study firstly confirmed the ability of nano-ZnO to reduce the oxidative effects generated by oxidative compounds and increased antioxidative activities, non-enzymatic antioxidants contents and possess excellent free radical scavenging activities (Siddiqi & Husen, 2017; Zafar et al., 2016). On the other hand, the use of nano-ZnO at high doses is not free of certain risks that should be assessed owing to its possible toxicity and its potential accumulation in feed and food that could mean its entrance to the food chain. One of the main causing mechanisms of the high toxicity of ZnO nanoparticles at high doses is its capacity to develop higher release of reactive oxygen species, including reactive oxygen and nitrogen species (ROS/RNS) and hydrogen peroxide (H_2O_2) in duckweed (Thwala, Musee, Sikhwivhilud, & Wepenerb, 2013).

Though the Deoxyribonucleic acid (DNA) is very stable or conservative in living plants and its primary structure is hardly changed, but it might get a heavy DNA damage due to the exposure to genotoxic stress which lead to the inhibition of DNA replication, transcription, or changes in the encoded proteins and consequently, complete inactivation of the encoded proteins (Maluszynska & Juchimiuk, 2005). So, many recent bioassays were developed to assess genotoxicity in plants and to provide reliable and robust results about the extent of the toxicity were applied such as flow cytometry, comet assay, and Random amplified polymorphic DNA polymerase chain reaction (RAPD-PCR) technique at the level of DNA.

Minute variations in nuclear DNA (nDNA) content, as well as DNA damage, in exposed plants were assessed by flow cytometry (FCM) which is a rapid, sensible and multiparametric and powerful technique

(Rodriguez, Azevedo, Fernandes, & Santos, 2011). Many reports have demonstrated the sensitivity of FCM technique, namely in detecting variations in nuclear DNA content and measurement of the clastogenic and genotoxic effects in dome plants such as *Allium cepa* exposed to X-ray radiation Carballo, Pincheira, and De La Torre (2006), lettuce and pea exposed to Cr(VI) (Monteiro et al., 2010; Rodriguez et al., 2011).

On the other hand, Single-cell gel electrophoresis (alkaline comet assay) is sensitive, a versatile, very appellative technique for estimation of DNA damages and capacity of DNA repair at the level of single cell to provide reliable and robust data regarding the clastogenicity of genotoxic agents such as radiation and others (Santos, Pourrut, & Ferreira de Oliveira, 2015). The comet assay allows fast detection of DNA damage and allows the determination of double- and single-stranded DNA breaks in a single cell and helps to measure the level of the migration of DNA from nuclei by using horizontal gel electrophoresis system (Pourrut, Pinelli, Celiz Mendiola, Silvestre, & Douay, 2015). Santos et al. (2015) reported that the comet assay have also been used to assess DNA damage in several parts of different plants such as roots, seeds, and fruits exposed to γ -irradiation and nanomaterials.

RAPD-PCR is used for DNA analysis in the field of genotoxicity (Pal, 2016). It is a highly sensitive method for the detection of genotoxicity and DNA damage induced by environmental pollutants like ionizing radiation. It is a sensitive and quite reproducible technique, capable of detecting variations in genome profiles, like normal band losses or appearances of new bands, when comparing DNA fingerprints from untreated and treated plants with genotoxic agents (Kecec, Sakcali, & Uzonur, 2010).

The present study aimed to investigate the radioprotective capacity of nano-ZnO in protecting of nuclear DNA of *Vicia faba* from damages induced by γ -radiation employing recent reliable and robust bioassays as flow cytometry, comet assay, and random amplified polymorphic DNA (RAPD) to evaluate the extent of damage and repair of DNA.

2. Material and methods

2.1. Plant material

Seeds of broad bean (*Vicia faba* variety Hsawi 2) were obtained from the King Saud University, College of Food Science and Agriculture, Department of Plant Production, Riyadh, Saudi Arabia. Fresh and healthy, uniformly sized seeds were surface sterilized in a 1% v/v solution of sodium hypochlorite by gentle magnetic stirring for 10 min, then rinsed three times with deionized water and air dried. These seeds were divided into four groups. The first group of seeds did not receive any further treatment to serve as the control. The second group was treated with

three concentrations of nano-ZnO, the third group irradiated with three doses of gamma (γ) radiation and the fourth group was nano-ZnO posttreatment of each dose of γ -irradiated seeds.

2.2. Gamma irradiation processes

Broad bean seeds were pre-soaked for 12 h distilled water at room temperature (25°C) and packed in high-density polyethylene bags and then irradiated with three different doses of gamma-rays (20, 50, 100 Gy: Gray) (Cobalt ⁶⁰ radiation source) from unit Gamma cell 220 No. 246 (Atomic Energy of Canada Ltd, Chalk River, ON, Canada); at the Research Center, College of Sciences, King Saud University. Non-irradiated seeds served as untreated samples (control).

2.3. Preparation of nano-ZnO suspensions

Nano-powder ZnO (purchased from M K Impex Corp, Canada), had average primary particle size, 50 nm, and purity, ≥ 99 . Three concentrations of nano-ZnO (500, 2000, and 4000 mg L⁻¹) were used in this study. After weighing of nano-powder, ZnO was dispersed and suspended directly in deionized Milli-Q water using mechanical stirrer. Small magnetic bars were placed in the suspension to stir and avoid aggregation followed by sonication on ice by ultrasonic vibration at 450 W, 40 kHz (UP100H Ultrasonic processor, Hielscher Ultrasound Technology, Germany), for 30 min and finally vigorous vortexing to obtain homogeneous suspensions for 5 min. *V. faba* seeds were treated with three concentrations of nano-ZnO for 24 h alongside untreated one.

2.3.1. Characterization of nano-ZnO suspension

Zinc oxide nanoparticles suspension was characterized for size and dispersity. To better understand the morphological characterization of the selected nano-ZnO, particle size distribution of the nanoparticles was determined through measurements carried out on Transmission Electron Microscopy (TEM) (JEOL JEM-2010, Japan, operated at 80 kV) images using Scion Image processing software at the Research Center, College of Sciences, King Saud University.

2.4. Combined effect between gamma-radiation doses and ZnO concentrations

Vicia faba seeds were exposed firstly to 20, 50 or 100 Gy γ -R doses and each dose immediately post-treated with three nano-ZnO concentrations (500, 2000, and 4000 mg L⁻¹) separately for 24 h to test the protective potential of nano-ZnO against γ -R induced DNA damage.

2.5. Evaluation of DNA status using DNA bioassays

According to the study of Sliwinska, Zielinska, and Jedrzejczyk (2005), seeds were used in this study instead of leaves to avoid the accumulation of staining inhibitors within leaves.

2.5.1. Estimation of nDNA content and genome size by flow cytometric technique

2.5.1.1. Isolation of nuclei suspensions. Nuclear suspensions isolated from untreated and treated broad bean seeds with nano-ZnO, γ -R, and ZnO post-treatments of γ -irradiated seeds were prepared according to Arumuganathan and Earle (1991). In brief, to release nuclei from seeds, 50 mg of germinated *V. faba* seeds were chopped with a sharp razor blade into <0.5 mm pieces in mixture of 1 mL of solution A (14.3 mL MgSO₄ buffer (ice-cold), 15 mg dithiothreitol (Sigma, D-0632), 300 μ L fluorochrome stain, propidium iodide (PI) stock, and 375 μ L Triton X-100 stock) in plastic petri dishes surrounding by ice. The homogenized nuclear suspension was then filtered through a 33 μ m nylon mesh into microcentrifuge tube, centrifugated at 15000 *g* for 15 to 20 s, and finally, the supernatant discarded. The pellet was then resuspended in 200 μ L of solution B (3 mL Solution A, 7.5 μ L RNAase (DNAase free), 3.0 μ L of human leucocytes (HLN)). At least 5000 nuclei per sample were analyzed using flow cytometry (LSRII and Sec: BL, Becton Dickenson) with an air-cooled argon-ion laser (15 mW operating at a wavelength of 488 nm).

2.5.1.2. Estimation of nuclear DNA content and genome size.

The measurements of relative fluorescence intensity of nuclei stained with propidium iodide (PI) were performed on a linear scale. The histogram of relative DNA content was obtained after the flow cytometric analysis of PI stained broad bean nuclei. Fresh HLN (2C = 7.0 pg) served as internal standards for PI flow cytometric analysis (Arumuganathan & Earle, 1991). The analysis compared the mean position of the peaks due to broad bean nuclei with the mean peak position of the internal standard. Fluorescence ratios (2C DNA content/sample), relative to the standard, were used to calculate DNA content (in picograms, pg) and the equivalent number of base pairs (genome size) was calculated assuming that 1 pg DNA is equivalent to 0.965 $\times 10^9$ bp or 965 Mbp according to (Dolezel, Bartos, Voglmayr, & Greilhuber, 2003) based on the following formulae:

$$\begin{aligned} &2C \text{ DNA content (pg)} \\ &= \frac{(\text{Sample peak mean} \times \text{Standard DNA content (7)})}{\text{Standard peak mean}}, \end{aligned} \quad (1)$$

where the symbol (C) (the DNA content of the haploid set of chromosomes).

2.5.2. Comet assay technique

2.5.2.1. Isolation of nuclei and preparation of their suspensions.

Isolation of nuclei and their suspension were carried out from untreated and treated *V. faba* seeds as described in the study of Abdelhaliem and Al-Huqail (2016) with some modifications. After removal of seed coat from treated and untreated *V. faba* seeds, embryonic tissues were placed in a petri dish containing 200 μ L of cold 400 mM Tris-HCl buffer, pH 7.5 (on ice) and gently sliced using a razor blade to release nuclei into the buffer under yellow light. The nuclei suspension was filtered through 50 μ m nylon mesh into microcentrifuge tube, then precipitated by centrifugation at 200 g for 5 min (4°C). The pellet was then resuspended in 200 μ L of Tris-MgCl₂ buffer. Each microscopic slide previously coated with 1% normal melting point agarose and dried at room temperature, was covered with a mixture of 55 μ L nuclear suspension and 55 μ L low melting point (LMP) agarose (1% prepared with phosphate-buffered saline) at 40°C and coverslipped. After at least 5 min, the slide was placed on ice and the coverslip was removed. Then, 110 μ L LMP agarose (0.5%) was placed on the slide and the coverslip was mounted. After 5 min on ice, the coverslip was removed. Slides of the alkaline SCGE with nuclei placed in a horizontal gel electrophoresis tank containing freshly prepared cold electrophoresis buffer (300 mM NaOH, 1 mM EDTA, pH > 13) (Juchimiuk, Gnys, & Maluszynska, 2006) and incubated for 15 min to allow the DNA to unwind prior to electrophoresis. Electrophoresis was performed at 26 V, 300 mA, for 30 min at 4°C. Next, the gels were rinsed three times with 400 mM Tris-HCl, pH 7.5 and stained with ethidium bromide (20 μ g/mL) for 5 min. After staining, the gels were dipped in ice-cold distilled water to remove the excess ethidium bromide and covered with a coverslip. All stages of comet assay were performed at room temperature and in dark conditions and all solutions were prepared freshly and used cool.

2.5.2.2. Imaging and analysis of DNA-lesions.

Immediately the images were captured, and DNA-lesions in 50 randomly selected nuclei on each slide were analyzed qualitatively and quantitatively using the fluorescence microscope (Olympus, Japan) with an excitation filter of BP 546/10 nm, a barrier filter of 590 nm, and a computerized CCD camera digital image analysis system (*Komet Version 3.1, Kinetic Imaging LTD*, Liverpool, UK). Tail moment (TM, integrated value of tail DNA density multiplied by the migration distance between the center of the head and the center of the tail) became a common descriptor and used as the primary measure parameter of DNA damage along with tail length (μ m) and percentage of DNA in the tail, tailed DNA (TD%, relative

percentage of DNA in the comet tail) Brugés and Reguero Reza (2007). The diameter of the nuclei was measured using Head Extent parameter of the software *Komet Version 3.1*. Fifty nuclei were measured for each treatment.

2.5.3. RAPD-PCR analysis

2.5.3.1. Isolation of genomic DNA.

Genomic DNA were isolated from untreated and treated *V. faba* seeds using a modified CTAB method as described in the study of Abdelhaliem and Al-Huqail (2016). DNA concentration was measured at 260 nm and by the ratio of A_{260/280} nm. The quality and yield of DNA was determined using 0.8% agarose gel electrophoresis stained with ethidium bromide; the bands were scored using a gel documentation system (Advanced American Biotechnology, Fullerton, CA, USA) and compared with those from a known standard lambda DNA marker.

2.5.3.2. DNA amplification by PCR using random RAPD primers.

Twenty random DNA oligonucleotide primers (10 mer) (Thermo Scientific) with variable nucleotide proportion (G-C content above 60–70%) were independently used in the PCR amplification process (UBC, University of British Columbia, Canada), following the method of Williams, Kubelik, Livak, Rafalski, and Tingey (1990) with some modifications as briefly described in the study of Abdelhaliem and Al-Huqail (2016). The PCR mixture contained 2.5 μ L 10X buffer and 15 mM MgCl₂ (Fermentas), with 0.25 mM each dNTP (Sigma), 0.3 μ M primer, 0.5 U Taq DNA polymerase (Sigma), and 50 ng template DNA. PCR was performed in a Palm Cycler apparatus (Corbett Research) using the following steps for 40 cycles: an initial denaturation of 4 min at 95°C followed by 1 min at 95°C, 1 min at 38°C, and 2 min at 72°C, with a final extension at 72°C for 5 min, and a hold temperature of 4°C at the end. The amplification products were electrophoresed on 1.5% agarose gel (Sigma) in TAE buffer (0.04 M Tris-acetate, 1 Mm EDTA, pH 8). The run was performed at 100 V for 1 h. Gels were stained with 0.2 mg/mL ethidium bromide for 15 min. The PCR products were visualized under a UV light transilluminator. A 100-bp DNA ladder (Gibco-BRL, USA) was used as the DNA size marker and loaded into the first lane of each gel to evaluate band size. Fractionated bands on the gel were detected by ethidium bromide fluorescence under UV-transilluminator and photographed using a gel documentation system (Bio-Rad, Hercules, CA, USA). All amplifications were repeated twice in order to confirm the reproducible amplification of scored fragments. Only reproducible and clear amplification bands were scored for the construction of the data matrix.

2.5.3.3. Data and DNA bands analyses. Gels were visualized with Photo Print (Vilber Lourmat, France) imaging system after the separation of PCR products by agarose gel electrophoresis, and digitized RAPD fingerprints were analyzed using one-dimensional software (Advanced American Biotechnology and Imaging, Fullerton CA 92831, USA) based on normal band losses, occurrences of new bands, the band intensity, the number of polymorphic (unique and non-unique DNA bands), and monomorphic DNA bands, and the molecular sizes of bands as well as band intensities for each samples. Amplified DNA products for RAPD analysis were scored based on the presence or absence of DNA bands for each primer. Polymorphism was evidenced as the presence and/or absence of DNA fragments between the samples. DNA band intensity revealed by RAPD analysis estimated by using image analysis software.

2.6. Statistical analyses

Statistical analysis was performed using one-way ANOVA followed by Bonferroni's multiple comparison test ($P < 0.05$) was used to test for significance between exposures. The obtained data were expressed as means \pm standard error (S.E.) of means (SEM, $n = 3$), if not differently indicated.

3. Results

3.1. Characterization of nano-ZnO

The interaction of nano-ZnO with cellular components based on the solubility and dispersion degree in their suspension. So, Figure 1 shows TEM images of distribution and dispersion of purified nano-ZnO suspension at three concentrations (500, 2000, and 4000 mg L⁻¹) at magnification power X150000. The variations in contrast and diameter of the nano-ZnO are mainly according to dose where they dispersed.

3.2. DNA bioassays

3.2.1. Flow cytometric bioassay

A detailed description of the action of nano-ZnO, γ -R, and nano-ZnO post treated γ -irradiated *V. faba* seeds were focused on isolated nuclei to estimate the extent of genotoxic action and alteration of nuclear DNA (nDNA) content and genome size alongside untreated one using flow cytometric (FCM) bioassay. Additionally, estimation of genome size per the chromosome number was investigated (Table 1 and Figures 2 and 3). The data obtained showed an increase in nuclear DNA content of γ -irradiated *V. faba* seeds after being treated with two nano-ZnO concentrations (500 and 2000 mg L⁻¹) which reached the value of 18.955 ± 0.050 and 20.190 ± 0.002 pg, respectively, when compared to that of the nuclei isolated from control samples (17.469 ± 0.008 pg). Meanwhile, the nuclear DNA content of the 4000 mg L⁻¹ nano-ZnO concentration decreased relative to the control group and reached 17.469 ± 0.008 pg.

In contrary, nDNA content and genome size of nuclei isolated from irradiated seeds with γ -R were in dose-dependent manner and scored a statistically significant reduction ($p < 0.5$) in nuclear DNA content at the 100 Gy (15.567 ± 0.005 pg) compared to that of the untreated nuclei which reached 17.469 ± 0.008 pg (Table 2 and Figure 3).

Data obtained in this study illustrated that γ -irradiated *V. faba* seeds post-treated with 500, 2000, and 4000 mg L⁻¹ nano-ZnO concentrations reduced the genotoxicity γ -R and increased the values of nDNA content and genome sizes compared to that of the equivalent γ -R doses prior treatment with nano-ZnO (Table 2). Post-treatment 2000 mg L⁻¹ nano-ZnO was the most ameliorative and protective dose of DNA against genotoxic action of dose-dependent γ -irradiation. This dose scored significantly maximum increasing of nDNA content which reached the value of (21.277 ± 0.077 pg) at 20 Gy γ -R compared to that of untreated one and equivalent of this γ -R dose prior treatment with nano-ZnO which reached the values of (17.469 ± 0.008 and 17.415 ± 0.04 pg, respectively) (Table 2 and Figure 3).

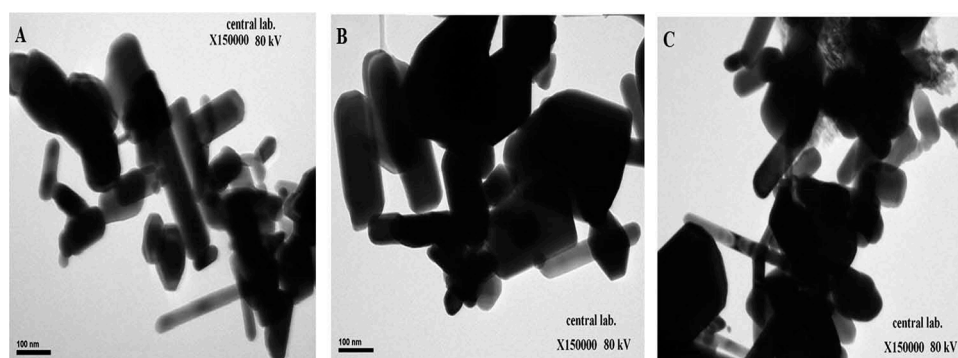


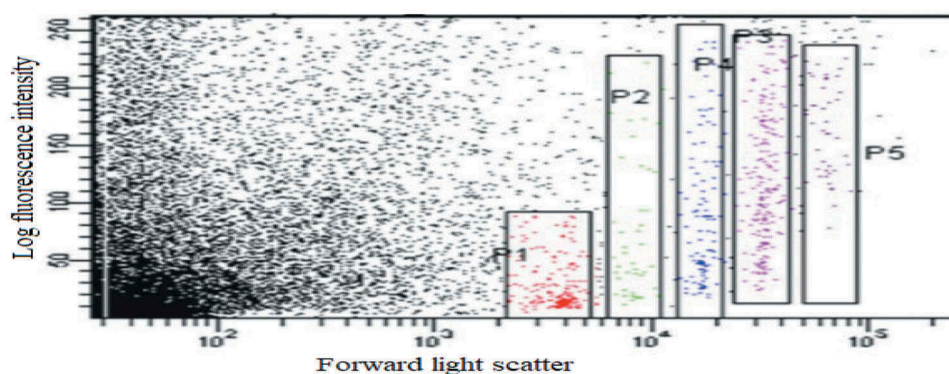
Figure 1. TEM micrographs at magnifications power X15000 of purified nano-ZnO suspension at three concentrations after dispersed in Milli-Q water. (a) 500 mg L⁻¹, (b) 2000 mg L⁻¹, and (c) 4000 mg L⁻¹.

Table 1. Nuclear DNA content and genome size of nuclei isolated from untreated and treated *V. faba* seeds with nano-ZnO, γ -R, and ZnO post-treatments of γ -irradiated seeds.

Treatments	Doses	Mean 2C nDNA content (pg)	1C genome size (Mbp)	Chromosome number	Genome size/chromosome number
Control	0.00	17.469 \pm 0.008	16858.27	2n = 12	1404.85
Nano-ZnO (mg L ⁻¹)	500	18.953 \pm 0.050	17327.00		1443.91
	2000	20.190 \pm 0.002 ^a	18190.24		1515.83
	4000	15.575 \pm 0.017	15030.19		1252.51
γ -R (Gy)	20	17.415 \pm 0.040	16806.34		1400.52
	Nano-ZnO posttreatments				
	R20/N500	17.529 \pm 0.027	16915.81		1409.65
	R20/N2000	21.767 \pm 0.077 ^a	21005.16		1750.43
γ -R (Gy)	50	16.863 \pm 0.022	16273.49		1356.12
	Nano-ZnO posttreatments				
	R50/N500	16.729 \pm 0.081	16143.99		1345.33
	R50/N2000	21.277 \pm 0.003 ^a	20532.31		1711.03
γ -R (Gy)	100	16.128 \pm 0.002	15569.31		1297.44
	Nano-ZnO posttreatments				
	R100/N500	15.567 \pm 0.005 ^a	15023.10		1251.92
	R100/N2000	17.955 \pm 0.003	17306.31		1442.19
γ -R (Gy)		20.054 \pm 0.055	19352.11		1612.68
		16.756 \pm 0.073 ^a	16169.54		1347.46

Results are expressed as mean \pm standard deviation of the mean (n = 3).

^a The mean difference is significant at the 0.05 level.

**Figure 2.** A five-parameter histogram of log intensity versus forward scatter generated by BD LSRII flow cytometer while analyzing the propidium iodide-stained for *V. faba* nuclei (2C) using human leucocytes (HLN) as internal standard (P1).

Based on the conversion of 1 pg = 965 Mbp, the genome sizes of treated *V. faba* nuclei were estimated. The values of genome size took the same trend as nDNA content ranging from (15023.10 Mbp) of 100 Gy γ -radiated nuclei to (20532.36 Mbp) of 20 Gy γ -irradiated *V. faba* seeds post-treated with 2000 mg L⁻¹ nano-ZnO dose. It was observed from the result obtained that the exposure to gamma irradiation dose-dependently caused a significant decrease in nuclear DNA content and increase in DNA damage while the nano-ZnO post-treatment of γ -irradiated *V. faba* seeds especially dose 2000 mg L⁻¹ attenuated this genotoxicity and protected DNA from damages (Table 1).

3.2.2. Comet assay

In the comet assay, nuclear DNA lesions with its breaks migrate toward the anode of electric field of electrophoresis generating comet-shaped DNA. Parameters of DNA lesions generated by comet assay based on the degree of DNA migration from the isolated nuclei and percentage of DNA in the tail, % of tailed DNA (TD%), relative percentage of DNA in the comet tail) and tail

moments (TM, integrated value of tail DNA density multiplied by the migration distance) as shown in Table 2. Figure 4 shows damages of nDNA of *V. faba* acquires the appearance of comet-shaped tail of DNA (damaged DNA or percent migrated DNA) with a head (undamaged DNA).

The data obtained in the current study illustrated significant variations in the extent of DNA damage in nuclei treated with high dose of nano-ZnO and three doses of γ -R in dose-dependent manner compared to control samples as well as nano-ZnO post-treatments of γ -irradiated *V. faba* seeds compared to equivalent of γ -R doses prior treatment with nano-ZnO; these variations reflect specific interference of each treatment based on the degree of genotoxicity and oxidative stress induced by it.

The highest DNA migration and increasing DNA damages were significantly evident at 100 Gy dose γ -irradiated nuclei where reached tailed ratio (20%), tail length (8.84 \pm 0.930 μ m), TD% (8.26 \pm 0.072), and TM (34.75 \pm 0.170) while the lowest one scored at 2000 mg L⁻¹ nano-ZnO dose which reached tailed ratio (2%), tail length (0.32 \pm 0.012 μ m), TD

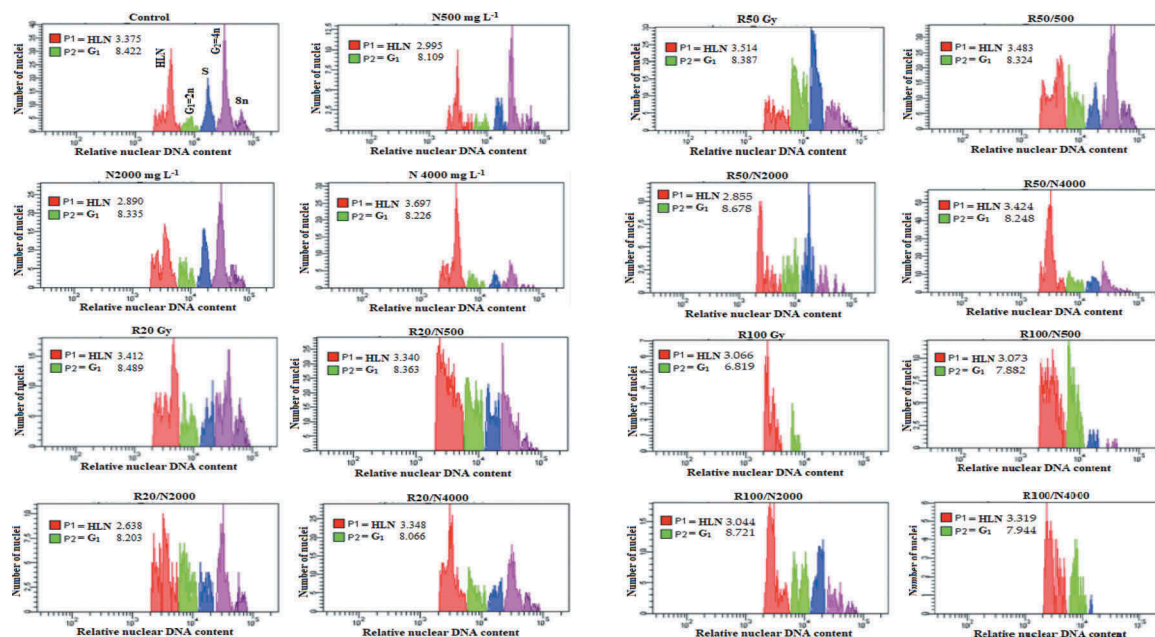


Figure 3. Flow cytometric analyses of nuclei isolated from untreated and treated *V. faba* seeds with nano-ZnO, γ -R, and ZO post-treatments of γ -irradiated seeds which chopped and then stained with propidium iodide. 2C nDNA content (pg) estimated at Gap₁ (G₁ = 2n) of interphase using peak position of the internal standard human leucocytes (HLN) (2C nuclear DNA content 7.0 pg) as internal standard. Red and green squares represent the mean peak positions of internal standard of fresh HLN and treated samples, respectively.

Table 2. Extent of nuclear DNA damage identified by single-cell gel electrophoresis (SCGE) of nuclei isolated from untreated and treated *V. faba* with nano-ZnO, γ -R, and nano-ZnO post-treatments of γ -irradiated seeds.

Treatments	Doses	Tail (damaged DNA) %	Head (undamaged DNA) %		Tail length (μ m)	Tailed DNA %	Tail Moment Unit
			Tail	Head			
Control	0.00	5	95		2.15 \pm 0.002	2.32 \pm 0.340	5.74 \pm 0.062
Nano-ZnO (mg L ⁻¹)	500	4	96		1.87 \pm 0.006 ^a	1.95 \pm 0.022	3.65 \pm 0.234
	2000	2	98		0.32 \pm 0.012 ^a	0.35 \pm 0.150 ^a	0.69 \pm 0.123 ^a
	4000	11	89		3.55 \pm 0.017	3.99 \pm 0.194	12.03 \pm 0.278
		15	85		3.88 \pm 0.091	3.65 \pm 0.044	16.65 \pm 0.205 ^a
Nano-ZnO post-treatments	R20/N500	8	92		3.79 \pm 0.028	3.61 \pm 0.512	7.16 \pm 0.154
	R20/N2000	6	94		2.51 \pm 0.024	2.67 \pm 0.089	5.79 \pm 0.061
	R20/N4000	12	88		3.94 \pm 0.054	3.54 \pm 0.335	10.47 \pm 0.142 ^a
Nano-ZnO post-treatments	R50/N500	10	90		2.82 \pm 0.056	3.42 \pm 0.143	13.682 \pm 0.054
	R50/N2000	8	92		3.58 \pm 0.083	2.54 \pm 0.098	7.47 \pm 0.040
	R50/N4000	13	87		4.05 \pm 0.162	4.65 \pm 0.056	18.80 \pm 0.267 ^a
Nano-ZnO post-treatments	R100/N500	12	88		3.22 \pm 0.066	4.31 \pm 0.065	15.13 \pm 0.322
	R100/N2000	11	89		3.79 \pm 0.055	3.61 \pm 0.120	12.24 \pm 0.034
	R100/N4000	15	85		5.88 \pm 0.091	5.53 \pm 0.044	27.65 \pm 0.205 ^a

Data are expressed as mean \pm standard deviation of the mean (n = 3).

^a The mean difference is significant at the 0.05 level.

% (0.35 \pm 0.150), and TM (0.69 \pm 0.123), following by 500 mg L⁻¹ of nano-ZnO dose which reached tailed ratio (4%), tail length (1.87 \pm 0.006 μ m), TD% (1.95 \pm 0.022), and TM (3.65 \pm 0.234) compared to the DNA migration from the control nuclei which was tailed ratio (5%), tail length (2.15 \pm 0.002 μ m), TD% (2.32 \pm 0.340), and TM (5.74 \pm 0.062).

The current data illustrated that γ -irradiated *V. faba* seeds post-treated with 500, 2000, and 4000 mg L⁻¹ nano-ZnO doses, especially 2000 mg L⁻¹, showed significant reduction of the DNA lesions induced by γ -radiation led to increasing repair and recovery of DNA compared to that of the equivalent γ -R doses prior

treatment with nano-ZnO (Table 2 and Figure 4). Most interestingly, comet parameters showed that 20 Gy γ -irradiated *V. faba* seeds post-treated with 2000 mg L⁻¹ nano-ZnO dose was the most ameliorative and protective dose of *V. faba* DNA against genotoxic action of γ -R. This dose showed significant reduction of DNA damages because it scored tailed ratio (6%), tail length (2.51 \pm 0.024 μ m), TD% (2.67 \pm 0.089), and TM (5.79 \pm 0.061) compared to that of equivalent of the 20 Gy γ -IR dose prior treatment with nano-ZnO which scored tailed ratio (13%), tail length (4.84 \pm 0.005 μ m), TD% (4.55 \pm 0.045), and TM (22.66 \pm 0.340) (Table 2 and Figure 4).

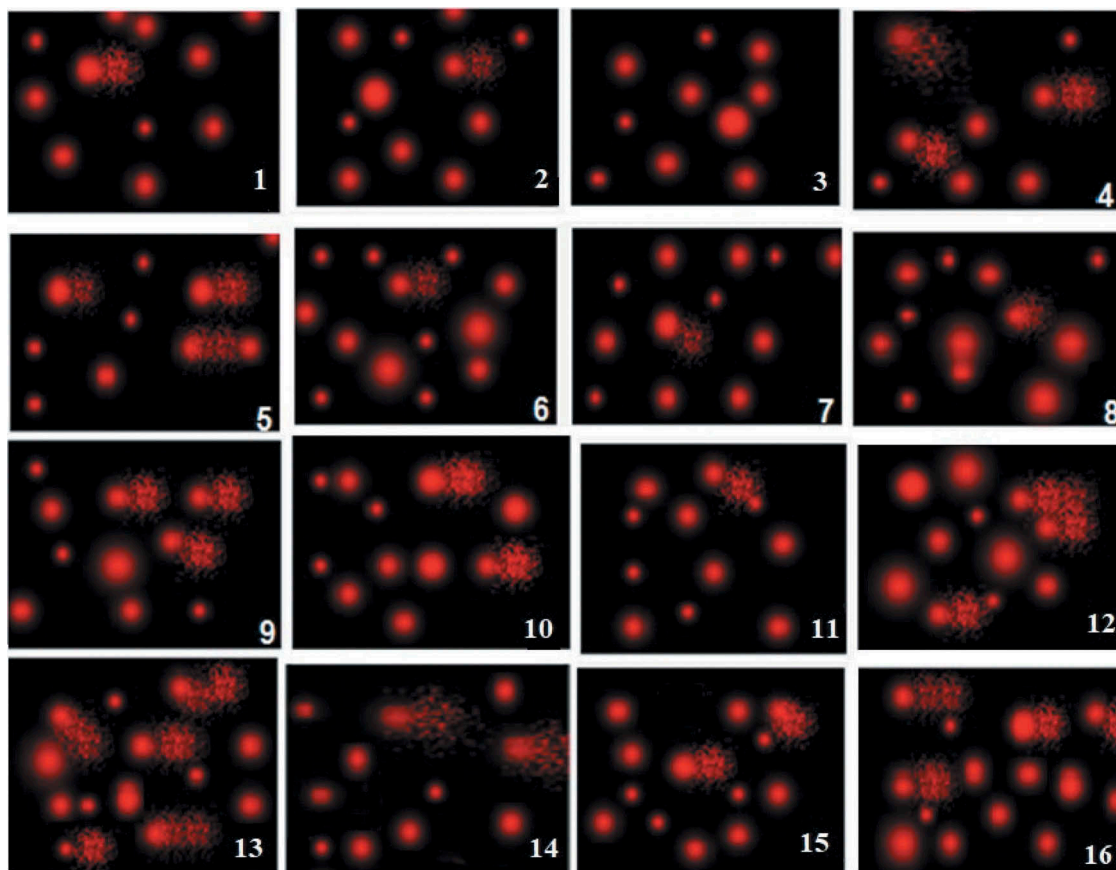


Figure 4. Comet images prepared by single-cell gel electrophoresis (SCGE) show the variable extent of nuclear DNA damage in the nuclei isolated from untreated and treated *V. faba* seeds. The images (1–16) represent control (1); nano-ZnO concentrations (2–4); γ -R (5, 9, and 13 for 20, 50, and 100 Gy, respectively); 6–8, 10–12, and 14–16 for 500, 2000, and 4000 nano-ZnO post-treatments of 20, 50, and 100 Gy γ -irradiated seeds, respectively.

3.2.3. RAPD-PCR bioassay

RAPD-PCR analysis was employed in the current study to estimate the extent of damage in DNA of *V. faba* treated with nano-ZnO, γ -R, and nano-ZnO posttreatment alongside untreated samples. Each treatment in addition to each primer exhibited distinctive quantitative and qualitative alterations in RAPD DNA banding pattern of treated samples compared to each other and to untreated ones. Twenty random primers were used for the RAPD analysis, in which only four primers of them (P-07, 09, 11, and 18) succeeded to generate prominent reproducible DNA bands and gave considerable results with many alterations in DNA banding pattern based on changes in bands number, bands size (bp), bands intensity, fractionation of some bands, appearance of new bands (unique bands) and disappearance of some bands (polymorphic bands) as shown in Tables 3 and 4 and Figure 5.

In total, 707 reproducible DNA bands were scored using the four primers (with an average of 177 bands/primer). Out of which, 312 polymorphic bands with value of 44.13% and 18 bands monomorphic bands (DNA bands appeared in all samples) with value of 2.55%. Out of polymorphic bands, 146 bands were unique (DNA band appeared in only one sample) with value of 20.65% and 166 bands were non-unique (DNA bands appeared in some samples and not others) value of

14.57%. Moreover, the total value of polymorphisms generated by four primers varied based on the presence or absence monomorphic band (Table 3). The highest value of DNA polymorphism generated by primer (P-18) and reached the value of (100%) owing to the absence of monomorphic bands among samples.

On the other hand, the highest number of gene products (268 bands) with value 37.91% was generated by primer-11, whereas the lowest number (103 bands) with value 14.57% was generated by the primer-18. Furthermore, the maximum number of gene products (58 bands) with value (8.20%) was observed at 20 Gy γ -irradiated seeds post-treated with 2000 mg L⁻¹ ZnO concentration compared to that of equivalent of the 20 Gy γ -IR dose prior treatment with nano-ZnO which scored (44 bands) with value (6.22%), Following this, the two nano-ZnO concentrations (2000 and 500 mg L⁻¹) scored 55 bands with value 7.78% and 54 bands with value 7.46%, respectively, compared to untreated samples which scored 52 bands with value 7.36%. Meanwhile, the minimum number of bands was (27) with value (3.82%) scored at 100 Gy compared to number of gene product at untreated one. This indicated that dose-dependent γ -R could disappear or lose genes from irradiated samples compare to that genes at control samples. On the other hand, nano-ZnO post-treatments

Table 3. RAPD-PCR amplification products of DNA isolated from untreated and treated *V. faba* seeds with nano-ZnO (N), γ -ray (R), and ZnO post-treatments of γ -irradiated seeds using four random primers using bio one D++ software (Vilber Lourmat, France).

Primer code	Primers sequences (5' → 3')	Amplicon Lengths (bp)	Total number of scorable bands in each Lane																Total bands	Polymorphic bands		Monomorphic bands		% of Polymorphism					
			Control				Nano-ZnO concentrations				Y-R dose				Y-R post ZnO					No	%	No	%						
			500 mg L ⁻¹	2000 mg L ⁻¹	4000 mg L ⁻¹	Control	20 Gy	50 Gy	100 Gy	R20/ N2000	R20/ N4000	R20/ N4000	R20/ N4000	Y-R post ZnO	Y-R post ZnO	Y-R post ZnO	Y-R post ZnO	Unique (U)							Total poly-morphic (U and non-U)				
P-07	GAA ACG GGT G	1739 – 75	10	7	12	12	9	11	14	13	13	8	11	13	9	6	10	10	9	164	23.20	23	3.25	51	7.21	4	0.57	92.73	
P-09	GGG TAA CGC C	1023 – 70	16	18	15	12	13	16	12	14	14	7	5	14	8	5	7	4	6	172	24.33	58	8.20	87	12.31	6	1.13	93.55	
P-11	CAA TCG CCG T	1000 – 90	20	20	21	17	16	20	22	21	14	17	17	12	10	12	15	14	268	37.91	47	6.65	84	11.88	8	1.41	91.30		
P-18	AGG TGA CCG T	989 – 98	6	9	7	7	6	8	10	9	4	4	4	3	5	6	7	8	4	103	14.57	18	2.55	90	12.73	0	0	100	
Overall total in each lane			52	54	55	48	44	55	58	57	33	37	47	34	27	36	37	33	707	707	100	146	20.65	312	44.13	18	2.55	94.55	
Total bands in all lanes			7.36	7.46	7.78	6.79	6.22	7.78	8.20	8.06	4.67	5.23	6.65	4.81	3.82	5.09	5.23	4.67											
% of total bands in each lane																													

could add or gain new genes and scored unique bands not found at control samples and scored large number of amplified DNA products than the equivalent.

Amplified DNA unique bands generated by 4 primers were varied among different treatments. The highest number of total unique bands (22 bands with value of 15.07%) was scored at 2000 mg L⁻¹ ZnO concentration while the lowest number (4 unique bands with value of 2.74%) were scored at 50 and 100 Gy of γ -ray. Meanwhile, 10 amplified DNA unique bands were generated by primer (P-09) at 2000 mg L⁻¹ ZnO concentration with amplicon lengths (921-858-851-688- 666-659- 600-482- 285-245 bp) while some treatments do not score any unique bands as shown in Table 4. Consequently, these unique bands can be used as biomarkers for these treatments.

4. Discussion

DNA damages in plant cells can be generated by reactive metabolites, spontaneously, and by mutations that occur during DNA replication and recombination processes or they can arise from exposure to environmental genotoxic agents (Tuteja, Ahmad, Panda, & Tuteja, 2009). Therefore, genotoxic events must be demonstrated using reliable and robust bioassays like flow cytometry, comet assay, RAPD-PCR.

Flow cytometry combined with comet assay and RAPD-PCR analysis could successfully detect genotoxic properties of high dose of nano-ZnO and γ -irradiation in dose-dependent manner as well as amelioration and repairing of damaged DNA induced by nano-ZnO post-treatments of γ - irradiated *V. faba* seeds.

Flow cytometry analysis detected significant variations in nuclear DNA content and genome size among nuclei isolated from untreated and treated seeds while comet assay detected the migration of damaged DNA from gel-embedded nuclei during electrophoresis. The more damaged nDNA analyzed by comet assay acquired the appearance of a comet, with more tail (damaged DNA). RAPD-PCR analysis detected DNA alteration and DNA damage inducing by genotoxic doses of treatments used by comparison of DNA amplification profiles generated from unexposed (control) and exposed (treated) samples and between exposed samples with each other's. This indicating the ability of these DNA bioassays to be powerful tools in genotoxicity testing.

Each treatment of nano-ZnO, γ -R, and nano-ZnO post-treatments scored specific interference with nDNA in dose-dependent manner. The data obtained showed increasing in nDNA content and genome size as revealed by flow cytometry beside significantly minimizing migration and damage of nDNA at γ - irradiated *V. faba* seeds post-treated with 2000 mg L⁻¹ nano-ZnO concentration compared to the equivalent γ -R doses prior treated nano-ZnO, followed by 2000

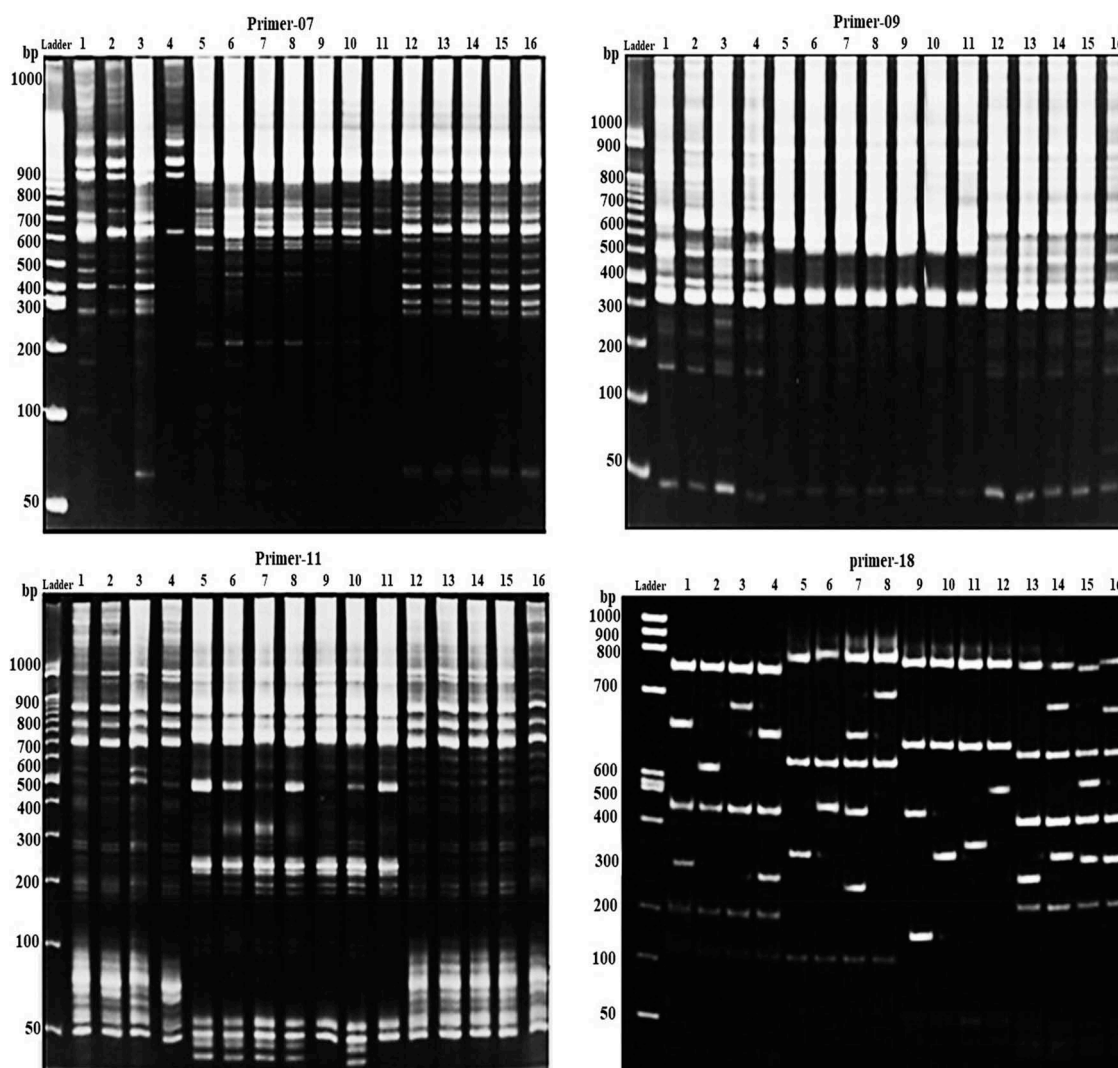


Figure 5. RAPD profiles of genomic DNA of *V. faba* generated by four random decamer primers. Lanes 1–16 represent the samples: control (1); nano-ZnO concentrations (2–4); γ -IR (5, 9, and 13 for 20, 50, and 100 Gy, respectively); lanes 6–8, 10–12, and 14–16 for 500, 2000, and 4000 nano-ZnO post-treatments of 20, 50, and 100 Gy γ -irradiated seeds, respectively.

and 500 mg L⁻¹ nano-ZnO concentrations compared to untreated one. The increasing nDNA contents by nano-ZnO treatments especially at 2000 mg L⁻¹ may be due to their ability to inducing doubling DNA and polyploidy in *V. faba* cells as evident by flow cytometry analysis or may be due to increasing antioxidant defense system in various *V. faba* cells by scavenging of free radicals providing adequate resistance to DNA for overcoming damage as evident by comet assay (Siddiqi & Husen, 2017; Zafar et al., 2016).

On the other hand, the high nano-ZnO dose (4000 mg L⁻¹) scored significant genotoxic action on nuclear DNA of *V. faba* led to the significant reduction of nDNA contents and increasing migration and lesions of nDNA. Nano-ZnO toxicity of *V. faba* plants induced by high concentrations may be due to its low dispersion in the suspension and its ability to promoting oxidative stress producing reactive oxygen species (ROS) which could induce DNA fragmentation and strand DNA breaks that lost from nuclei of *V. faba* and consequently, the high dose led to reducing of nDNA

content and increasing DNA lesions (Thwala et al., 2013). Other interpretation of toxicity of high nano-ZnO dose (4000 mg L⁻¹) may be due to dissolution of nano-ZnO particles in *V. faba* cells after entrance through seed coat or their accumulation onto external surfaces of seeds causing aggregation of particles resulting in clogging of pores which an interrupted water uptake and delay the entrance of water through seed coat leading to increasing cellular oxidative stress, accumulation of harmful reactive oxygen species (ROS), and reduction of antioxidant defense system and consequently, DNA damage (Thwala et al., 2013).

In contrast, the current study showed a dose-dependent relationship between γ -radiated seeds and major DNA damages. High 100 Gy dose exhibited heavy DNA damages causing extensive reduction of nuclear DNA content and increasing of migration and lesions of DNA from nuclei compared to untreated one. This proved that γ -irradiation is a potent DNA-damaging agent causing changes in DNA which may be

intragenic changes such as (point mutations within a gene sequence) or intergenic changes such as (inversions, deletions, duplications, translocations of DNA) (Caplin & Willey, 2018) or inducing a higher frequency of chromosome damage associated with sticky chromosomes, fragmentation of whole chromosomes and chromosome segregation errors during mitosis and meiosis resulting in unequal distribution of the DNA in the daughter cells and consequently, variation in nDNA content in the two newly formed cells (Abdelhaliem, Abdullah, & AL-Huqail, 2013; Potapova & Gorbysky, 2017).

On the other hand, γ radiation may be induced different types of DNA lesions owing to their interaction with cellular DNA directly by deposition of energy in cells and/or indirectly by generating free radical formations as radiolytic reactive oxygen species (ROS). These DNA lesions including single and double DNA strand breaks, deletion or insertion of base pairs, base pair damage and DNA cross-links which led to critical DNA lesion and chromosome breaks (Caplin & Willey, 2018). Therefore, these radio-lesions of DNA may lead to the reduction of nuclear DNA content and consequently, the size of genome of irradiated *V. faba* cells.

Based on the data revealed by RAPD analysis, it can be said that each treatment may lead to specific-level genotoxic stress and specific interference with nuclear DNA of *V. faba*. The results of RAPD analysis were performed by considering the bands (genes) which appear in the control sample are the criterion of the judgment while polymorphism observed in RAPD profiles included losing of some of control bands and appearance new other bands.

The current data observed distinctive alterations in the DNA fingerprint (RAPD banding patterns) that may reflect DNA alterations in the genomic DNA which ranges from single base changes (point mutations), small insertion and deletion to complex chromosomal rearrangements (Lal, Mistry, Shah, Thaker, & Vaidya, 2011). These DNA alterations generated highly levels of DNA polymorphisms between control and treated *V. faba* based on deletion or losing normal DNA bands at toxic doses of γ -radiation and high dose of nano-ZnO as evident from the lowest number of DNA bands at these doses compared to untreated one or addition or gaining new other bands produced by the selected primer sets especially at 2000 mg/L⁻¹ nano-ZnO dose pre and post-treated of irradiated seeds as evident from highest number of newly amplified DNA bands at these treatments. These variation in DNA profile patterns may be due to the presence/absence of priming sites, priming complementary or the distance between priming sites (Liu et al., 2005).

The polymorphisms between control and treated *V. faba* can be explained on the basis of biological way by which γ rays and nano-ZnO treatments, in dose-

dependent manner, interacts with DNA, by producing their own ROS through the indirect and/or direct effect on *V. faba* DNA or the ability of toxic doses in inducing of structural changes in the sequences of genomic DNA such as DNA breakage, base pair deletions, large genomic DNA rearrangements, DNA adducts, point mutations, transpositions inversions, and translocations within base pair sequences of DNA resulting in the loss or gain of DNA bands and consequently, generation of different DNA lengths and high level of polymorphisms (Dhakshanamoorth, Selvaraj, & Chidambaram, 2011). The polymorphisms may alter the distance between two annealing sites and delete an existing site of new one or reflection of variation in gene expression which can be a better parameter to measure the pattern of genetic variations between treatments. This indicating that DNA polymorphism detected by RAPD-PCR analysis offered a useful molecular bioassay for the identification of DNA damage induced in gamma radiation treated plants.

The variations in sizes of DNA bands between treatments revealed by RAPD analysis may be due to separate loci which are scored on basis the base of amplification (present) and non-amplification (absent) of DNA fragment through PCR cycles while variation in the number of amplified DNA bands may be due to the direction and number of base-pair sequences within the genomic DNA are complementary to the primer sequence (Dhakshanamoorth et al., 2011). Meanwhile, variation in DNA band intensity may be resulting from competition between PCR products, product copy number differences of amplified DNA lengths, heterozygosity, partial mismatching or comigration of primer sites that leads to the production of shorter and longer DNA amplified fragments (Lal et al., 2011).

Furthermore, the presence of new bands (unique) may be due to a change in the priming sites leading to new annealing events or due to large deletions and homologous recombination could lead to the appearance of new bands. On the other hand, lost or gained RAPD bands revealed RAPD analysis may be due to point mutations, inversions, deletions, additions or gross chromosomal rearrangements affect the presence/absence of primer sites, their complementarity to primers and/or the distance between priming sites (Lal et al., 2011).

The most exciting in this study, γ - irradiated *V. faba* seeds post-treated with three doses of nano-ZnO showed significant reduction of DNA damage depending on both nano-ZnO concentrations and γ -R doses. The current study interpreted the mechanism by which nano-ZnO protect DNA from damages induced by γ -R may be due to their ability to prevent the accumulation of ROS generated by γ -R when entrance *V. faba* cells by virtue their antioxidant properties which led to increasing antioxidant nuclear defense system of *V.*

faba cells (Siddiqi & Husen, 2017; Zafar et al., 2016), providing DNA adequate resistance against oxidative damage and DNA fragmentation induced by γ -rays and consequently, increasing the viability of DNA.


5. Conclusion

In conclusion, three DNA bioassays (flow cytometry, comet assay, and RAPD-PCR) in combination could successfully showed the positive and improvement effect of 2000 and 500 mg L⁻¹ nano-ZnO doses on *V. faba* DNA and radioprotective efficiency of nano-ZnO post-treatments in increasing the viability and resistance of DNA against oxidative damages induced by γ -ray. Thus, the study suggests that the positive and promotor doses of nano-ZnO should be utilized to develop ecofriendly and effective as 'nano-fertilizers' while nano-ZnO post-treatments used as nano-radioprotective agents for the protection of economic crop plants and improvement of their yield and quality.

Disclosure statement

No potential conflict of interest was reported by the authors.

ORCID

Ekram Abdelhaliem Mohamed  <http://orcid.org/0000-0002-9007-5158>

Hanan Fahad A. L. Harbi  <http://orcid.org/0000-0002-4653-8717>

Nagwa Aref  <http://orcid.org/0000-0001-8672-0989>

References

- Abdelhaliem, E., Abdullah, H., & AL-Huqail, A. A. (2013). Oxidative damage and mutagenic potency of fast neutron and UV-B radiation in pollen mother cells and seed yield of *Vicia faba* L. *BioMed Research International*, 2013, 1–12.
- Abdelhaliem, E., & Al-Huqail, A. A. (2016). Detection of protein and DNA damage induced by elevated carbon dioxide and ozone in *Triticum aestivum* L. using biomarker and comet assay. *Genetics and Molecular Research*, 15, 1–19.
- Arumuganathan, K., & Earle, E. D. (1991). Estimation of nuclear DNA content of plants by flow cytometry. *Plant Molecular Biology Reporter*, 9, 229–233.
- Brugés, K., & Reguero Reza, M. T. (2007). Evaluación preliminar de toxicidad, genotoxicidad y actividad antimicrobiana de *Sida rhombifolia* L. *Revista Colombiana De Biotecnología*, 9, 5–13.
- Caplin, N., & Willey, N. (2018). Ionizing radiation, higher plants, and radioprotection: From acute high doses to chronic low doses. *Frontiers in Plant Science*, 9, 847–866.
- Carballo, J. A., Pincheira, J., & De La Torre, C. (2006). The G2 checkpoint activated by DNA damage does not prevent genome instability in plant cells. *Biological Research*, 39, 331–340.
- Dhakshanamoorth, D., Selvaraj, R., & Chidambaram, A. L. (2011). Induced mutagenesis in *Jatropha curcas* L. using gamma rays and detection of DNA polymorphism through RAPD marker. *Comptes Rendus Biologies*, 334, 24–30.
- Dolezel, J., Bartos, J., Voglmayr, H., & Greilhuber, J. (2003). Nuclear DNA content and genome size of trout and human. *Cytometry*, 51, 127–128.
- Duhan, J. S., Kumar, R., Kumar, N., Kaur, P., Nehra, K., & Duhan, S. (2017). Nanotechnology: The new perspective in precision agriculture. *Biotechnology Reports (Amsterdam)*, 15, 11–23.
- Iqbal, M. (2016). *Vicia faba* bioassay for environmental toxicity monitoring: A review. *Chemosphere*, 144, 785–802.
- Jiang, J., Pi, J., & Cai, J. (2018). The advancing of zinc oxide nanoparticles for biomedical applications. *Bioinorganic Chemistry and Applications*, 2018, 1–18.
- Juchimiuk, J., Gnys, A., & Maluszynska, J. (2006). DNA damage induced by mutagens in plant and human cell nuclei in acellular comet assay. *Folia Histochemica Et Cytobiologica*, 44, 127–131.
- Karami, M., Asri-Rezaei, S., Dormanesh, B., & Nazarizadeh, A. (2018). Comparative study of radioprotective effects of selenium nanoparticles and sodium selenite in irradiation-induced nephropathy of mice model. *International Journal of Radiation Biology*, 94, 17–27.
- Kekec, G., Sakcali, M. S., & Uzonur, I. (2010). Assessment of genotoxic effects of boron on wheat (*Triticum aestivum* L.) and Bean (*Phaseolus vulgaris* L.) by using RAPD analysis. *Bulletin of Environmental Contamination and Toxicology*, 84, 759–764.
- Lal, S., Mistry, K. N., Shah, S. D., Thaker, R., & Vaidya, P. B. (2011). Genetic diversity assessment in nine cultivars of *Catharanthus roseus* from Central Gujarat (India) through RAPD, ISSR and SSR markers. *Journal of Biological Research*, 1, 667–675.
- Liu, W., Li, P. J., Qi, X. M., Zhou, Q. X., Zheng, L., Sun, T. H., & Yang, Y. S. (2005). DNA changes in barley (*Hordeum vulgare*) seedlings induced by cadmium pollution using RAPD analysis. *Chemosphere*, 61, 158–167.
- Liu, Y., Zhang, P., Li, F., Jin, X., Li, J., Chen, W., & Li, Q. (2018). Metal-based nanoenhancers for future radiotherapy: Radio-sensitizing and synergistic effects on tumor cells. *Theranostics*, 8, 1824–1849.
- Ma, T.-H., Owens, E., & Cabrera, G. L. (2005). Genotoxic agents detected by plant bioassays. *Reviews on Environmental Health*, 20, 1–13.
- Maluszynska, J., & Juchimiuk, J. (2005). Plant genotoxicity: A molecular cytogenetic approach in plant bioassays. *Arh Hig Rada Toksikol*, 56, 177–184.
- Monteiro, M. S., Rodriguez, E., Loureiro, J., Mann, R. M., Soares, A. M., & Santos, C. (2010). Flow cytometric assessment of Cd genotoxicity in three plants with different metal accumulation and detoxification capacities. *Ecotoxicology and Environmental Safety*, 73, 1231–1237.
- Nurmansyah, S., Alghamdi, S., Hussein, M., & Farooq, M. M. (2018). Morphological and chromosomal abnormalities in gamma radiation-induced mutagenized faba bean genotypes. *International Journal of Radiation Biology*, 94, 174–185.
- Pal, S. (2016). Detection of environmental contaminants by RAPD method. *International Journal of Current Microbiology and Applied Sciences*, 5, 553–557.
- Potapova, T., & Gorbysky, G. J. (2017). The consequences of chromosome segregation errors in mitosis and meiosis. *Biology (Basel)*, 6, 12.
- Pourrut, B., Pinelli, E., Celiz Mendiola, V., Silvestre, J., & Douay, F. (2015). Recommendations for increasing alkaline comet assay reliability in plants. *Mutagenesis*, 30, 37–43.
- Reisz, J. A., Bansal, N., Qian, J., Zhao, W., & Furdui, C. M. (2014). Effects of ionizing radiation on biological molecules-

- mechanisms of damage and emerging methods of detection. *Antioxid Redox Signal*, *21*, 260–292.
- Rodriguez, E., Azevedo, R., Fernandes, P., & Santos, S. (2011). Cr(VI) induces DNA damage, cell cycle arrest and polyploidization: a flow cytometric and comet assay study in *Pisum Sativum*. *Chemical Research in Toxicology*, *24*, 1040–1047.
- Santos, C. L., Pourrut, B., & Ferreira de Oliveira, J. M. (2015). The use of comet assay in plant toxicology: Recent advances. *Frontiers in Genetics*, *6*, 216.
- Siddiqi, K. S., & Husen, A. (2017). Plant response to engineered metal oxide nanoparticles. *Nanoscale Research Letters*, *12*, 92.
- Sliwinska, E., Zielinska, E., & Jedrzejczyk, I. (2005). Are seeds suitable for flow cytometric estimation of plant genome size? *Cytometry Part A*, *64A*, 72–79.
- Thwala, M., Musee, N., Sikhwivhilud, L., & Wepenerb, V. (2013). The oxidative toxicity of Ag and ZnO nanoparticles towards the aquatic plant *Spirodela punctata* and the role of testing media parameters. *Environmental Science Processes & Impacts*, *15*, 1830–1843.
- Tuteja, N., Ahmad, P., Panda, B. B., & Tuteja, R. (2009). . Genotoxic stress in plants: Shedding light on DNA damage, repair and DNA repair helicases. *Mutation Research*, *681*, 134–149.
- Veronica, N., Guru, T., Thatikunta, R., & Reddy, N. S. (2015). Role of Nano fertilizers in agricultural farming. *International Journal of Environmental Science and Technology*, *1*, 1–3.
- Wang, C., Blough, E., Dai, X., Olajide, O., Driscoll, H., Leidy, J. W., ... Wu, M. (2016). Protective Effects of Cerium Oxide Nanoparticles on MC3T3-E1 Osteoblastic Cells Exposed to X-Ray Irradiation. *Cellular Physiology and Biochemistry*, *38*, 1510–1519.
- Williams, J. G. K., Kubelik, A. R., Livak, K. J., Rafalski, J. A., & Tingey, S. V. (1990). DNA polymorphisms amplified by arbitrary primers are useful as genetic markers. *Nucleic Acids Research*, *18*, 6531–6535.
- Xie, Y., He, Y., Irwin, P. L., Jin, T., & Shi, X. (2011). Antibacterial activity and mechanism of action of zinc oxide nanoparticles against *Campylobacter jejuni*. *Applied and Environmental Microbiology*, *77*, 2325–2331.
- Zafar, H., Ali, A., Ali, J. S., Haq, I. U., & Zia, M. (2016). Effect of ZnO nanoparticles on *Brassica nigra* seedlings and stem explants: Growth dynamics and antioxidative response. *Frontiers in Plant Science*, *20*, 535.